FINAL REPORT

STRUCTURAL STUDY OF BISMUTH AND TIN BORATE GLASSES USING ELECTRON DIFFRACTION TECHNIQUE

Nattapol Laorodphan

Maejo University

July 2020

FINAL REPORT

STRUCTURAL STUDY OF BISMUTH AND TIN BORATE GLASSES USING ELECTRON DIFFRACTION TECHNIQUE

Nattapol Laorodphan

Maejo University

July 2020

Contract No. TRG5780137

Final Report

Structural Study of Bismuth and Tin Borate Glasses Using Electron Diffraction Techniques

Nattapol Laorodphan

Maejo University

Project Granted by the Thailand Science Research and Innovation and Maejo University

บทคัดย่อ

รหัสโครงการ TRG5780137

ชื่อโครงการ การศึกษาโครงสร้างแก้วบิสมัทบอเรตและดีบุกบอเรตด้วยเทคนิคการเลี้ยวเบนของอิเล็กตรอน

ชื่อนักวิจัย ณัฐพล เลาห์รอดพันธุ์

อีเมล์ Nattapol.lao@gmail.com

ระยะเวลาโครงการ 1 มิถุนายน 2557 – 25 กรกฎาคม 2563

งานวิจัยนี้เน้นการศึกษาเชิงโครงสร้างของแก้วระบบบอเรตซึ่งมีโบรอนออกไซด์เป็นองค์ประกอบ ได้แก่แก้วที่มีการเติมดีบุกออกไซด์ บิสมัทออกไซด์ และวานาเดียมออกไซด์ที่มีการเจือลิเทียมออกไซด์ โดยใช้เทคนิคต่าง ๆ ได้แก่ จุลทรรศนศาสตร์อิเล็กตรอน และรามานสเปกโทรสโกปี การเตรียมตัวอย่างทำได้โดยการผสมวัตถุดิบต่างๆ ที่ให้ออกไซด์ตามต้องการและหลอมที่อุณหภูมิสูง 1000 องศาเซลเซียส และทำให้เย็นตัวอย่างรวดเร็วที่อุณหภูมิห้องระหว่างแผ่นโลหะเหล็กกล้าไร้สนิม 2 แผ่น เมื่อได้ตัวอย่างเก็บในโถดูดความชื้นเพื่อใช้ในการวิเคราะห์เชิงโครงสร้างต่อไป ผลการวิจัยพบว่าไม่สามารถเตรียมแก้วระบบดีบุกบอเรตได้เนื่องจากยังไม่สามารถควบคุมบรรยากาศการหลอมได้ดีทำให้ดีบุกเกิดปฏิกิริยากับออกซิเจนในอากาศที่ผิวแก้วทำให้ไม่สามารถผลิตแก้วเนื้อเดียวได้ ในแก้วระบบบิสมัทบอเรตพบว่าสามารถเตรียมแก้วได้เป็นส่วนใหญ่ ยกเว้นระบบที่มีองค์ประกอบของบิสมัทสูง จากวิเคราะห์ด้วยเทคนิคการเลี้ยวเบนของรังสีเอ็กซ์พบว่าชิ้นงานที่เป็นแก้วมีความเป็นอสัณฐาน โดยแก้วมีความหนาแน่นที่เพิ่มขึ้นเมื่อปริมาณของบิสมัทออกไซด์เพิ่มขึ้น อย่างไรก็ตามเมื่อนำไปคำนวณปริมาตรเชิงโมลพบว่าปริมาตรเชิงโมงลดลงและเพิ่มขึ้น ทั้งนี้เนื่องมาจากการเปลี่ยนแปลงโครงสร้างแก้ว จากการศึกษาด้วยการวิเคราะห์ตัวอย่างแก้วด้วยภาพถ่ายจุลทรรศนอิเล็กตรอนกำลังขยายสูง พบว่าตัวอย่างที่นำไปวิเคราะห์มีความเป็นอสัณฐานสูง โดยไม่พบการเรียงตัวของระนาบอะตอม อย่างไรก็ตามการศึกษาด้วยการเลี้ยวบนของอิเล็กตรอนจากเทคโนโลยีและซอฟแวร์ที่มีอยู่ยังมาสามารถให้ข้อสรุปได้เนื่องจากยังไม่สามารถเปลี่ยนแปลงความเข้มของอิเล็กตอนไปเป็นระยะห่างระหว่างอะตอม

ได้ อีกทั้งผลการศึกษาที่สำคัญจากเทคนิครามานสเปกโทรสโกปีนั้นพบว่าโครงสร้างหน่วยย่อยของโบรอนชนิดที่มีออกซิเจนล้อมรอบ 3 อะตอมลดลง ซึ่งเห็นได้ชัดจากการลดโครงสร้างของวงแหวนโบรอกซอล สำหรับแก้วระบบลิเทียมวานาเดียมบอเรตที่มีการเจือลิเทียมออกไซด์นั้น พบว่าไม่สามารถผลิตแก้วที่มีความเป็นอสัณฐานได้ทั้งหมด โดยในแก้วทุกองค์ประกอบที่ศึกษาพบมีผลึกขนาดเล็กระดับนาโนปะปนอยู่จากภาพถ่ายจุลทรรศนอิเล็กตรอนกำลังขยายสูง ซึ่งพบการจัดเรียงตัวของอะตอมที่เป็นระเบียบเกิดเป็นระนาบขึ้นแม้ในองค์ประกอบที่มีวานาเดียมต่ำ ซึ่งสอดคล้องกับผลที่ได้จากแบบรูปการเลี้ยวเบนของรังสีเอ็กซ์ที่พบพีคของแบรกก์ที่ตำแหน่ง 13.8 และ 28.3 องศา โดยเฉพาะอย่างยิ่งในตัวอย่างที่มีวานาเดียมออกไซด์ในปริมาณสูง อีกทั้งยังสามารถยืนยันด้วยภาพถ่ายจุลทรรศนอิเล็กตรอนกำลังขยายสูง ซึ่งพบการจัดเรียงตัวของอะตอมที่เป็นระเบียบเกิดเป็นระนาบขึ้นแม้ในองค์ประกอบที่มีวานาเดียมต่ำ ค่าความหนาแน่นของแก้วชนิดนี้เพิ่มขึ้นตามปริมาณวานาเดียมออกไซด์ที่เพิ่มขึ้น อย่างไรก็ตามพบว่าค่าปริมาตรเชิงโมลก็มีค่าสูงขึ้นเช่นกันโดยคาดว่าเกิดจากการที่โบรอนส่วนมากอยู่ในสภาพแวดล้อมชนิดที่มีออกซิเจนล้อมรอบ 4 อะตอม ซึ่งสอดคล้องจากผลการวิเคราะห์ด้วยเทคนิครามานสเปกโทรสโกปีที่ไม่พบโครงสร้างของวงแหวนโบรอกซอล

คำสำคัญ โครงสร้างแก้ว การเลี้ยวเบนของอิเล็กตรอน จุลทรรศนอิเล็กตรอน
รามานสเปกโทรสโกปี

ABSTRACT

Project Code TRG5780137

Project Title Structural Study of Bismuth and Tin Borate Glasses Using Electron Diffraction Techniques

Investigator Nattapol Laorodphan

E-mail Address Nattapol.lao@gmail.com

Project Period June 1st, 2014 – July 31st, 2020

This research focused on structural study of borate glasses, in which boron oxide was used as one of the ingredients. Tin oxide, bismuth oxide and vanadium oxide with lithium oxide doping were added to the interested borate glasses in this study. Electron microscopy and Raman spectroscopy were used as main characterization methods. Glass samples were prepared by mixing raw materials, which provide those needed oxide, melting at 1000 °C and quenching to room temperature between two stainless steel plates. The samples were kept in desiccator to prevent moisture attack prior to characterization. The results showed that homogenous tin borate glasses could not be prepared due to the fact that the atmospheric condition was not fully controlled. Thus, tin oxide was oxidized by remaining oxygen in the furnace. In bismuth borate glasses, most of the samples with high bismuth content were successfully prepared. The X-ray diffraction study revealed that the samples were amorphous. The density values of glasses increased as bismuth oxide content increases. However, anomaly of molar volume was detected, which could be due to the change of glass structure. The analysis from high resolution electron image also confirmed the amorphous nature of glass samples, in which the lattice fringes could not be observed. However, inconclusive result was obtained from electron diffraction technique due to the limitation of the interpretation technology and software for electron density to atomic distance conversion. Moreover, Raman spectra showed the reduction of 3-coordinated boron as the intensity of the peak corresponding to boroxol ring reduced. For lithium oxide

doped vanadium borate glasses, all samples were partially crystallised as the nano crystallites were observed in the sample by high resolution electron images. The crystallite was detected even in low vanadium content glasses. This was supported by the presence of Bragg's peak at about 13.8 and 28.3 degree of the X-ray diffraction patterns of the samples, especially samples with higher vanadium content. Density values of the lithium doped vanadium borate glasses increased as vanadium oxide content increases. However, the molar volumes of the glasses also increased. This may be due to the higher concentration of 4-coordinated boron in the glass structure, which corresponds to the absence of boroxol ring peak of Raman spectra.

Keywords Glass Structure, Electron diffraction, Electron microscopy, Raman spectroscopy

Executive summary

1. Introduction to Research

Nonlinear optical properties of materials are important in the development of some optical devices, for instance an optical switching, Raman amplifier and laser, and supercontinuum generation fibre optics. These nonlinear optical responses are also found in glasses containing lead oxide (PbO) or bismuth oxide (Bi_2O_3) [1, 2]. It was found that the nonlinear optical properties in glass material depend on the content of these two additive oxides (Lead and bismuth oxides) as the higher nonlinearity were in higher heavy metal oxide content glasses. Lead and bismuth ions in the +2 and +3 oxidation states, respectively, have a lone pair of electrons. Other examples of lone pair cations are Tl^{+}, Sn^{2+}, Sb^{3+} and Te^{4+} [3]. Addition of oxide containing these ions in the glass could introduce the nonlinearity of the optical properties. However only two oxides, i.e. bismuth oxide (Bi_2O_3) and tin oxide (SnO) are of interest in this study because of it is more environmental friendly compound as the other lower-oxidation state cations (Tl^{+} and Pb^{2+}) are toxic. However, tin containing glass melting process requires a control atmosphere (nitrogen atmosphere) in a carbon crucible due to the disproportionation reaction of tin.

Addition of lone pair cation in a network of glass former, such as B_2O_3 SiO_2 GeO_2, causes the breaking down of the glass network and also the changes in structural environment of the glass network. The B_2O_3 and GeO_2, for example, undergo changing in their local boron and germanium environment from lower oxygen-coordinated to higher oxygen-coordinated environment as the additive oxide (i.e. lone pair cation oxide) content increases. On the other hand, SiO_4 network in silica glass remains four-oxygen-coordinated environment, with different number of bridging oxygen (Si-O-Si bond in the network). The number of bridging oxygen is scaled with the additive oxide content as the Si-O-Si bonds are broken. The changes in the structural environments of network of glass former can be observed

using various techniques, for example solid-state nuclear magnetic resonance (NMR), X-ray or neutron diffraction and electron diffraction. Boron oxide (B_2O_3) is used as a glass former in this study.

It was also found that the changes in local environments of the lone pair cation are varied depending on the content of lone pair cation oxide in the glass. For instance, Hannon et al (2009) reported that a mixture of high coordinated Sn-O units and asymmetric, low coordinated Sn-O units (which may be in a trigonal pyramid of SnO_3) presents in low tin oxide content borate glasses, while only low coordinated Sn-O units are predominated in high tin oxide borate glasses [4]. However, the reported structures of lone pair cation in oxide glass, found in the literatures, remain unclear as the structures were obtained from an ambiguous analysis, e.g. by comparing the experimental results with crystalline structure. Thus, it is very challenging to examine accurately the local structure of this lone pair cation in oxide glass, in order to predict or control the nonlinear optical properties of glass. The lone pair cation oxides selected for this study are bismuth oxide (Bi_2O_3) and tin oxide (SnO).

The difficulty in identifying the local structure of lone pair cation in oxide glass does not only arise from the instrumentation perspective, but also the material itself. Achieving the homogeneity of structure or composition throughout the glass sample is very difficult. In a large-scale melting, such as in the glass making factory, some processes, e.g. milling and mixing, are necessary for making a homogeneous composition of the glass product [5]. In contrast, the smaller scale like in the laboratory or an experimentally scale experiences a lot more difficulty. However, it was assumed that standing the melt at about 100 $^{\circ}$C above their liquidus temperature for several hours could introduce the homogeneity of the glass. Thus, the glass in this research will be prepared by traditional melt-quench method using a soaking time at melting temperature, which depends on the composition of glass, for a couple hour.

Various techniques have been applied to the investigation of structure of amorphous (glass) material, for instance, infrared and Raman spectroscopy, solid-state NMR and neutron diffraction. The studies of glass structure using infrared and Raman spectroscopy revealed some useful information mainly on the glass former sites (B, Si or Ge), leaving somehow the unsolved structure of the cation

additive sites. Although the local structure of cation sites has been ambiguous revealed by solid-state NMR and neutron diffraction studies, the equipment could not be easily accessed in Thailand. Electron diffraction, which are available in Thailand, could be used to investigate the glass structure, revealing the information on the local environments of network former and modifier cation. Thus, the electron diffraction technique will be mainly used in this project. However, to maintain the reliability of the information obtained from the electron diffraction, other techniques such as Raman spectroscopy and solid-state NMR will also be used for comparison.

Other difficulties in structural study of amorphous materials are sample preparation for transmission electron microscopy (TEM), typically use jet electropolishing or ion milling, and the working conditions, i.e. electron accelerating voltage. All the parameters involving in sample polishing stage (in this experiment, the ion milling will be used) or electron diffraction experimental stage have to be controlled, so that the structure information obtained could be a representative of the whole sample, which means that there are no structure changes during both stages.

2. Literature Review

Optical glasses that have been used in the optical switching devices and the optical fibre possess the nonlinear optical properties. Lead-borate (PbO-B_2O_3) [1, 6], bismuth-borate (Bi_2O_3-B_2O_3) [1, 2, 7], lanthanum aluminium silicate (La_2O_3-Al_2O_3-SiO_2) [8] and lithium telluride germinate (Li_2O-TeO_2-GeO_2) [9] glasses have been reported to have the nonlinear optical properties. The nonlinear optical properties do not exist in alkali or alkali earth containing glasses. This may be due to the lone pair effects. The above-mentioned systems contain cation oxide that particularly have a lone pair of electrons when forming bond, i.e. PbO, Bi_2O_3, La_2O_3 and TeO_2. The nonlinearity of the optical properties were reportedly scaled with the chemical composition of the glass, in which it increases with the increasing amount of lone pair cation oxide [1]. The bismuth oxide (Bi_2O_3) and tin oxide (SnO) are chosen as glass modifiers in this study due to the lower toxicity compare with lead oxide (PbO).

From the glass systems above the main network of the glass composes of a so called “glass former”, which in general are SiO_2, GeO_2, B_2O_3 and P_2O_5. All interesting system that has been reported contains SiO_2, GeO_2 and B_2O_3 oxide work as a glass network. SiO_2 and GeO_2 oxides could be melted at a very high temperature compare with the B_2O_3, which has a lower melting temperature. Moreover, the borate glass (B_2O_3 containing glass) is more interesting due to the presence of the anomalous behaviour, which reflexes the structure-properties relationship, and the existing of boron superstructural units, for example boroxol ring, triborate and tetraborate. Boron superstructural units were also found to be depended on the glass composition. Thus, bismuth and tin borate glasses with different amount of lone pair cation oxide contents will be examined.

The structure of alkali and alkali earth borate glasses has widely been studied using various techniques including solid-state NMR [10], neutron diffraction or scattering techniques [11] and Raman spectroscopy [12]. The results reveal that conversion of [BO_3] units, found in pure B_2O_3 glass, to [BO_4] units as alkali or alkali earth oxide content increases up until about 33 mol% of alkali oxide in the glass. The maximum concentration that gives the highest number of [BO_4] units may change depending on type of alkali and alkali earth oxide. In this region (under 33 % additive content, which is equivalent to about 0.5 mole fraction of alkali oxide in B_2O_3 glass), the total number of [BO_4] units, so called “N_4 values”, is increasing as a function of alkali content as shows in **Figure 1** [13] in lithium borate glasses. Beyond this point, in alkali or alkali earth borate glass, the disruption of [BO_4] formation is due to the formation of non-bridging oxygen (B-O-B bonds are broken) causing the continuous reduction of [BO_4] units in the glass as appears in **Figure 1**. This behaviour of local environment of boron unit changing when the alkali oxide or alkali earth oxide is added to the glass is so called “borate anomaly”.

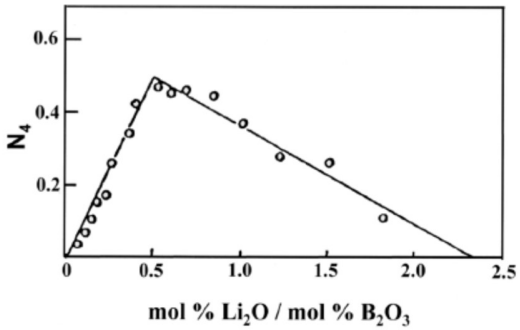

Figure 1 fraction of [BO_4] units in the lithium borate glass as a function of Li_2O content.*[from [13]]*

However, the borate anomaly is somehow different in lone pair cation containing borate glasses, for example thallium borate glass, as the N_4 values or the number of [BO_4] units seem to be suppressed at a high lone pair cation oxide content, causing the constant of N_4 value as shows in **Figure 2**.

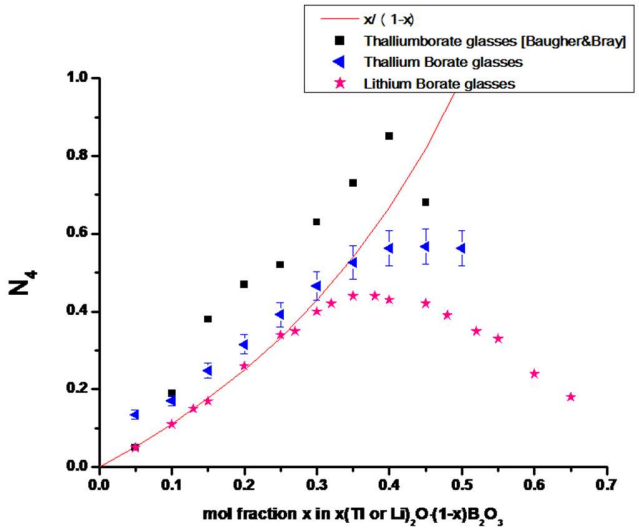

Figure 2 N_4 values of thallium borate glasses reveal the steadiness of N_4 values at 0.35 to 0.50 comparing with the lithium borate glasses (star). *[from [14]]*

It was also found that the amount of fourfold coordinated boron atoms; [BO_4] in bismuth borate glass at 31 – 67 mol% Bi_2O_3 does not significantly change, which is in consistent with thallium borate glasses containing 35 to 50 mol% of thallium oxide. Moreover, the broad maximum of N_4 values covering a

range from 40 to 70 mol% of Sb_2O_3 in antimony borate glasses, where all N_4 values is about 0.1 [15]. However, the explanation of this strange N_4 behaviour in lone pair cation containing borate glasses remains unclear. The assumption that has been used to explain this behaviour is the effect of lone pair of electrons that could stabilise the [BO_4] units [14], unlike other alkali or alkali earth borate glasses, in which the non-bridging oxygen atoms were created.

The local environments of lone pair cation in oxide glasses seem to change with the glass composition as the mixture of high and low coordinated lone pair cations presents in low lone pair cation oxide content glasses, whereas the only low coordinated cations were observed in high lone pair cation oxide content glasses, i.e. found in thallium germanate and borate glasses [16, 17], tin silicate glass [18] and tin borate glass [4]. Changes in the coordination number of lone pair cation is relevant to a hybridisation of the valence electron orbital involved in bonding [14]. If only s^2 lone pair of electrons is involved, no strong effects from the hybridization on the environment of the cation, the lone pair of electrons is then sterically inert. In this case, the symmetric high coordinated cations are observed as shows from an example of thallium germanate glasses in **Figure 3a**. On the other hand if the lone pair of electrons is sterically active (where p and d orbital are involved in the hybridization), all oxygen atoms is then forced to locate on the same side of the cation atom, as a results asymmetric low coordinated environment is then observed (**Figure 3b**). However, no absolute coordination number has been reported. The reported results were obtained from the comparison of the coordination number of cation in glass and the crystalline phase at the corresponding composition. The accurate coordination number of cation will then be very useful information in order to understand the effects of this lone pair of electrons on the glass structure.

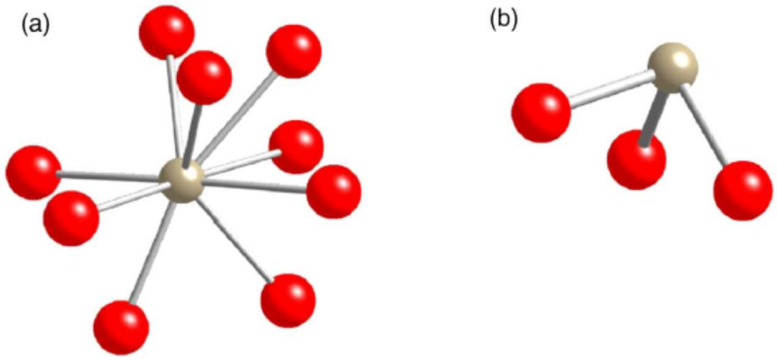

Figure 3 a) symmetric high coordinated environment and **b)** asymmetrical low coordinated environment thallium proposed for thallium germanate glasses [16].

The structure of bismuth borate glasses, which is one of the interesting system in this study, has been investigated using neutron diffraction [19] and ^{11}B solid-state NMR [20]. The borate anomaly presents in this glass with the maximum of N_4 value about 0.46 at the range of Bi_2O_3 content between 40 to 50 mol%. However, the local environments of bismuth have not been investigated. The similarity was observed in tin borate glasses, studied by solid-state NMR and neutron diffraction [4]. The borate anomaly was also observed as the $[BO_4]$ units increase as SnO increases revealing the maximum of N_4 value. Tin environments also changed as a function of SnO content, in which the symmetric high coordinated tin environment is found in low SnO content glasses. In high tin oxide content glasses, an asymmetric low coordinated tin environment presented. Although a slightly contamination from Al_2O_3, as alumina crucible was used for glass melting, was detected. So that in this study, the carbon crucible will be used for tin glass melting in a nitrogen atmosphere in order to eliminate the effect of Al_2O_3 on the glass structure.

Electron diffraction studies of amorphous material has been widely used to study the metallic glasses [21]. Low amount of publications on the studies of covalent amorphous materials has been published, although some have been reported [22]. The most relevant literature is on the study of short-

range order in telluride borate glasses using electron diffraction techniques studied by Bursukova *et al* [23], in which the distances between B-O and Te-O have been resolved. The distances between these pair of atoms could be used to calculate the coordination number of the oxygen atoms surrounding revealing the local environment of lone pair cation in these glasses. The TEM sample thickness for electron diffraction experiment was about 500 Å. The diffraction pattern was recorded at 80 kV, which is quite low electron acceleration, as the higher acceleration voltage may change the structure of glass during the experiment. Incoherent electron scattering was then eliminated to get better background for analysis. The radial distribution function (RDF) could then be calculated from the coherent scattering of the electron by Fourier transformation. The RDF, which could be converted to the total correlation function; T(r), of the glass correlates to the atomic distances between pair of atoms as demonstrates in **Figure 4**.

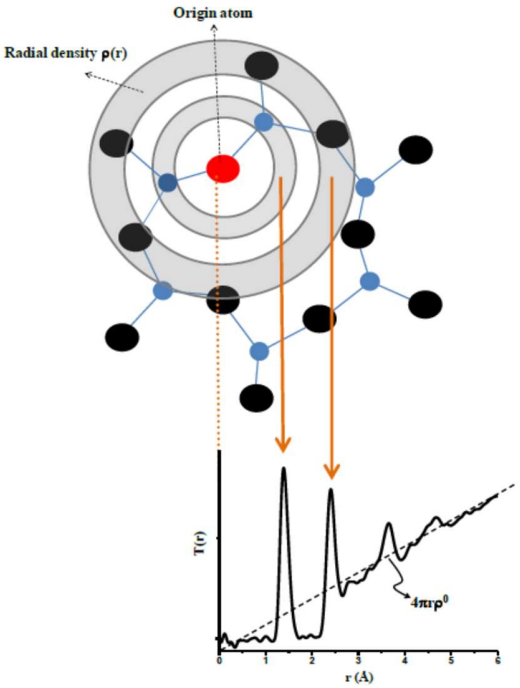

Figure 4 The relationship between T(r) and the real space of atomic distance in glass observed by diffraction technique. [*from [14]*]

It should be noted that thin sample preparation techniques, e.g. ion milling and electropolishing [21], and TEM working condition are concerned as the structure of glass may change during these stages [21, 24]. The electropolishing and ion milling techniques may change the structure. However, preparation of sample with care may reduce a risk of structure changes during this preparation period. Kestel (2000) [25] proposed the preparation methods used to polished the inorganic glass samples using jet polishing techniques. Sun *et al* (2005) also report the condition that the artificial feature was not produced during sample preparation method.

3. Objective

To investigate the structural change of the amorphous samples at various concentration of oxide additives

4. Research Methodology

4.1 Conventional melt-quench method will be used for glass preparation. The quenching was done between two stainless steel plates.

4.2 Selected xSnO-$(1-x)$$B_2O_3$, $x$$Bi_2O_3$-$(1-x)$$B_2O_3$ and $x$$V_2O_5$-$(1-x)$$LiBO_2$ composition were melted in a platinum crucible at 1000 ^{o}C for 30 minutes. The melts were then pulled out and rapidly cooled to room temperature between two stainless steel plates.

4.3 Samples were then examined by X-ray diffractometer in order to investigate the degree of crystallinity of the samples.

4.4 Glass samples were then crushed to very small pieces to be thin enough for transmission electron microscopy investigation.

4.5 Ring diffraction patterns of all glass samples will then be collected.

4.6 The electron diffraction patterns will then be scanned, and its electron intensity will be collected using ImageJ software. Intensity profile was then compared.

4.7 Density of the samples was measured using Archimedes' method, using xylene as a liquid media to prevent the moisture attack. Molar volume of the sample was then calculated using the following relationships shown in Equation 1.

$$MV = MW/\rho \qquad \text{(Eq.1)}$$

where MV is molar volume (cm^3/mol)

ρ is density of the sample (g/cm^3)

MW is glass molecular mass (g/mol)

4.8 Raman spectroscopy was then used for structural analysis, where bonding between various atoms in the samples will be revealed.

Results

1. Tin Borate Glasses

Seven batches of tin oxide and boron oxide mixture at different tin contents were weighed to receive the nominal composition as shown in **Table 1**.

Table 1 Nominal composition of Tin borate composition.

CODE	mol fraction SnO	mol fraction B_2O_3
SnB5	0.05	0.95
SnB15	0.15	0.85
SnB25	0.25	0.75
SnB35	0.35	0.65
SnB45	0.45	0.55
SnB55	0.55	0.45
SnB65	0.65	0.35

Disproportionation reaction of tin oxide during melting may cause the inhomogeneity of glasses. Thus, the melting process should be done in vacuum condition or in a controlled atmosphere. The modification of tube furnace was the needed for atmospheric controlling during melting as shown in **Figure 5**.

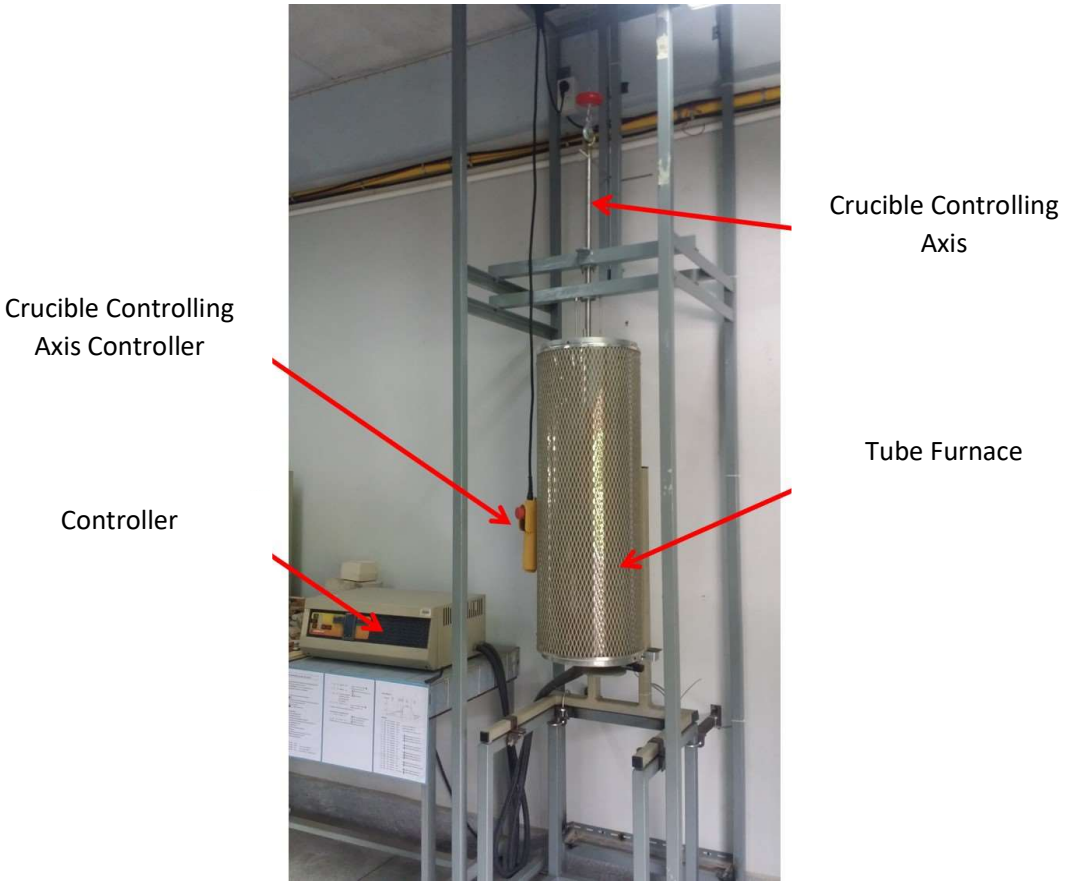

Figure 5 Modified tube furnace for atmospheric controlling

Even though the use of atmospheric controlled tube furnace during melting, the sample preparation was not achieved as showed in **Figure 6**. Thus, characterizations were not continued for these sample.

Figure 6 Partially crystallised glass sample in tin borate system (SnB15)

2. Bismuth Borate Glasses

Six batches of bismuth oxide and boron oxide mixture at different tin contents were weighed to receive the nominal composition as shown in **Table 2**.

Table 2 Nominal composition of Tin borate composition.

CODE	mol fraction Bi_2O_3	mol fraction B_2O_3
BiB15	0.15	0.85
BiB25	0.25	0.75
BiB35	0.35	0.65
BiB45	0.45	0.55
BiB55	0.55	0.45
BiB65	0.65	0.35

All six compositions could be melted homogeneously. However, only five composition (BiB25 – BiB65) could be cooled to obtain amorphous samples with difference shade of colour as described in **Table 3.** It was found that the higher intensity of yellowish colour increased as bismuth oxide content increased. Further characterization was done only on clear samples only.

Table 3 The presence of bismuth borate sample

CODE	Chemical Formula	Presence	CODE	Chemical Formula	Presence
BiB15	$0.15Bi_2O_3 \cdot 0.85B_2O_3$	-Inhomogeneous -Partially crystallised	BiB45	$0.45Bi_2O_3 \cdot 0.55B_2O_3$	-Homogeneous -Clear glass -Yellowish (level 3*)
BiB25	$0.25Bi_2O_3 \cdot 0.75B_2O_3$	-Homogeneous -Clear glass -Yellowish (level 1*)	BiB55	$0.55Bi_2O_3 \cdot 0.45B_2O_3$	-Homogeneous -Clear glass -Yellowish (level 4*)
BiB35	$0.35Bi_2O_3 \cdot 0.65B_2O_3$	-Homogeneous -Clear glass -Yellowish (level 2*)	BiB65	$0.65Bi_2O_3 \cdot 0.35B_2O_3$	-Homogeneous -Clear glass -Yellowish (level 5*)

*The intensity of yellowish colour ranks from 1 – 5, in which the larger the number, the darker the colour.

Weight loss of the samples was also monitored by considering the weight difference before and after melting. It was suggested that weight loss could be due to the evaporation of some liquid component during melting. This could be the lower melting point component, which is boron oxide (450 $^{\circ}$C). Thus, the calculated after melt composition would be done based on the loss of boron oxide content in glasses. The percent weight loss and the calculated composition were shown in **Table 4**. However, the nominal composition was used instead as the weight loss is only 2 %. As a result, %mole of Bi_2O_3 was not far off the nominal composition. It was revealed that the sample with highest boron oxide (BiB25) content had largest weight loss, which support the assumption that the loss is due to the evaporation of low melting point component.

Table 4 Percent weight loss of the samples and estimated bismuth oxide content in the samples.

CODE	% mole Bi_2O_3	% mole B_2O_3	Total weight loss (g)	Percent weight loss	% mole Bi_2O_3 (estimate from weight loss)
BiB25	25.00	75.00	0.2634	2.64	24.28 – 26.71
BiB35	35.00	65.00	0.1070	1.07	34.69 – 36.16
BiB45	45.00	55.00	0.0839	0.84	44.75 – 46.39
BiB55	55.00	45.00	0.0718	0.72	54.80 – 56.69
BiB65	65.00	35.00	0.0646	0.06	64.84 – 67.04

Density of glass samples was measured using Archimedes principle, where the weight of sample in air (Wt_{air}) and weight of sample in liquid medium ($Wt_{imersed}$) were required. In this experiment

xylene was used as a medium, in which its density is 0.85012 g/cm^3 at the testing temperature (32.8 $^{\circ}$C). The density values and molar volumes of glass sample revealed in **Figure 7**. It was found that density increased as bismuth oxide content increases. This may be due to the increase of higher density component, i.e. bismuth oxide (8.9 g/cm^3), comparing to the lower density of boron oxide. The molar volumes of glasses also increased as bismuth oxide content increases. However, when comparing to the molar volume of boron oxide glass (~38 cm^3/mol), the borate anomaly was suggested to be occurred in these glasses. Thus, the change of glass structure was then expected.

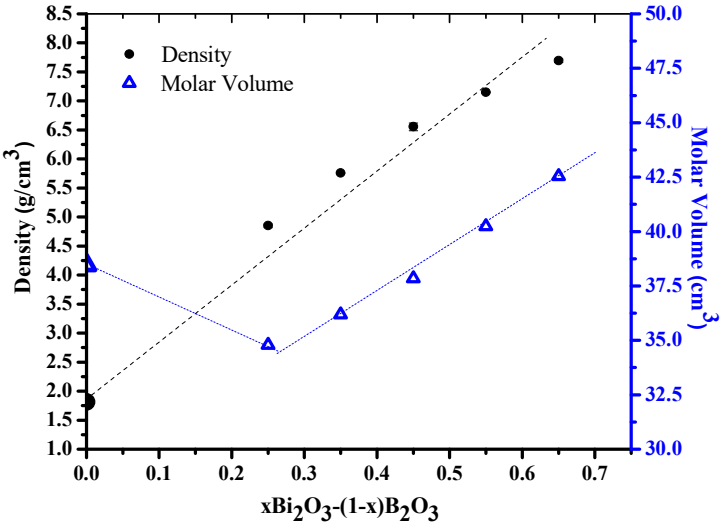

Figure 7 Density and molar volume of glasses

X-ray diffraction patterns of glass samples shows in **Figure 8**, which confirm the presence of amorphous nature of glass sample. No corresponding Bragg's peak was detected. On the other hand, broad patterns were detected as expected. Moreover, the amorphous nature of the sample can be confirmed by the high-resolution electron image (**Figure 9**) collected by transmission electron microscopy techniques. Homogeneous atomic distribution was revealed without any phase separation or lattice fringe.

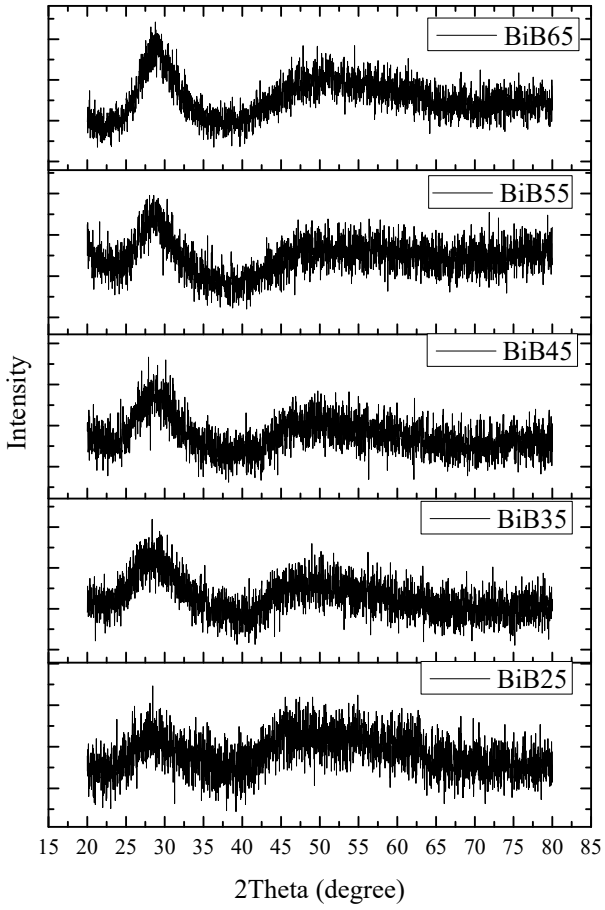

Figure 8 X-ray diffraction patterns of all glass samples.

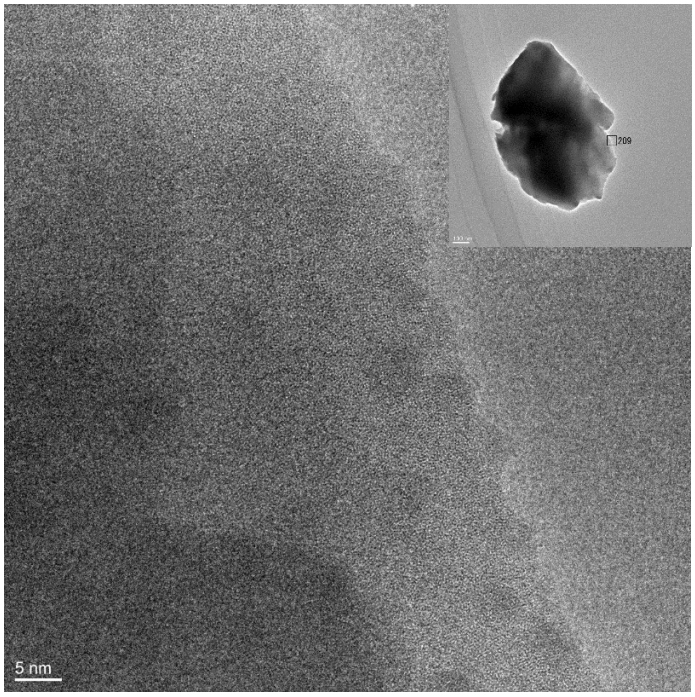

Figure 9 High-magnification TEM images of BiB65 glass sample.

Diffraction pattern of all glass samples were collected using transmission electron microscope. The hallow patterns were observed confirming that the diffracted electrons were from an amorphous sample. The selected area diffraction patterns were then shown in **Figure 10**. It was found that difference intensity of electron (brighter zone) could be observed. Moreover, the length of the hallow pattern from the middle spot was also different. However, the electron density and distance interpretation from ImageJ software (**Figure 11**) was not good enough for further analysis.

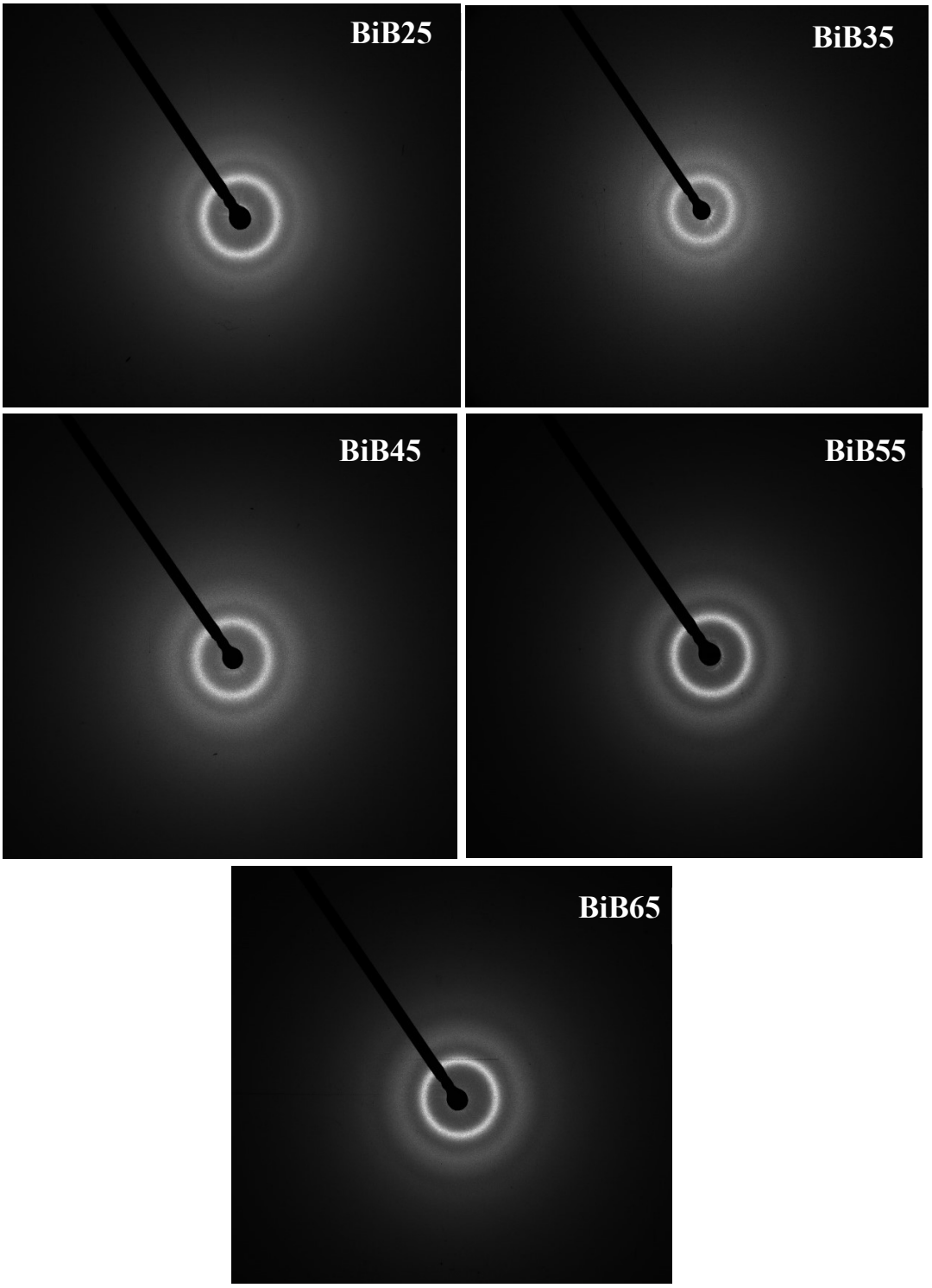

Figure 10 Hallow pattern of bismuth borate glasses obtained from transmission electron microscopy

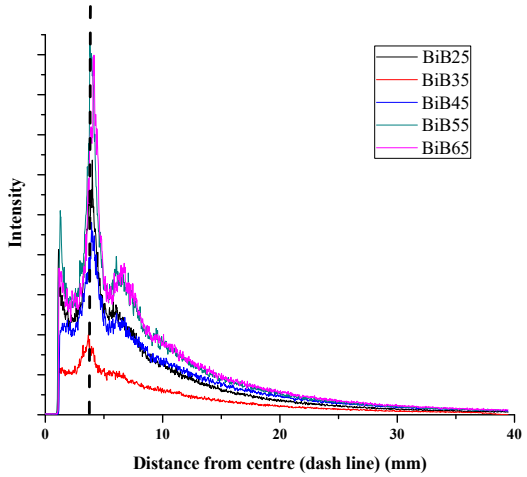

Figure 11 Electron density and distance profile of hallow patterns shown in Figure x. Dash line indicates the position of the middle spot.

Raman spectroscopy was then also supporting the structural investigation of the sample. The laser wavelength used in this research was 532 nm. It was found that the structure of glasses changes as the composition of glass changes as shifting and changing of the Raman peaks were observed. The spectra show in **Figure 12**. The important peak positions found in the spectra were also listed in **Table 5**. The results revealed that addition of bismuth oxide caused the change of boron environment in the glass structure. As can be seen from lowest bismuth oxide containing glass (BiB25), boroxol ring, triborate, pentaborate and diborate, which contain [BO_3] units were detected. As bismuth oxide content increasing, the peak related to [BO_3] structure started to reduce and eventually disappear and *vice versa*.

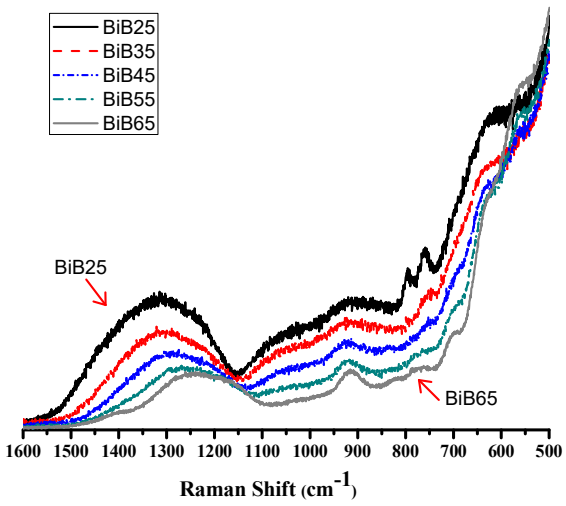

Figure 12 Raman spectra of bismuth borate glasses.

Table 5 Raman shift with its corresponding assignments.

Raman Shift (cm^{-1})	**Peak shape**	**Assignement**	**$[BO_3]$: $[BO_4]$ ratio**	**Detected sample**
760	Sharp	Triborate / Pentaborate	2 : 1 / 4 : 1	BiB25
800	Sharp	Boroxol ring	3 : 0	BiB25
900	Broad	n/a	-	Every sample with different concentration
1200	Broad	Diborate	2 : 2	Every sample with different concentration
1400	Broad	Non-bridging oxygen in $[BO_4]$	-	Every sample with different concentration

3. Lithium Vanadium Borate Glasses

Six batches of bismuth oxide and boron oxide mixture at different tin contents were weighed to receive the nominal composition as shown in **Table 6**. Lithium metaborate ($LiBO_2$) glass was prepared prior to the mixing with vanadium oxide make samples. The weight change of the samples was monitored to determine composition loss.

Table 6 Composition of lithium doped vanadium borate samples

Code	Chemical Formula	Molar present of V_2O_5	Molar percent of $LiBO_2$
0.35V-0.65LB	$0.35V_2O_5 \cdot 0.65\ LiBO_2$	35	65
0.40V-0.60LB	$0.40\ V_2O_5 \cdot 0.60\ LiBO_2$	40	60
0.45V-0.55LB	$0.45\ V_2O_5 \cdot 0.55\ LiBO_2$	45	55
0.50V-0.50LB	$0.50\ V_2O_5 \cdot 0.50\ LiBO_2$	50	50
0.55V-0.45LB	$0.55\ V_2O_5 \cdot 0.45\ LiBO_2$	55	45
0.60V-0.40LB	$0.60\ V_2O_5 \cdot 0.40\ LiBO_2$	60	40

The samples were dark and non-transparent as shown in **Figure 13**. Thus, the presence of crystallinity or amorphous nature of samples were necessarily examined by X-ray diffraction (miniFlex, Rigaku) using Cu-Kα irradiation source, determining from 10 – 55 degree with step size of 5.33 degree/min. The results (**Figure 14**) shown that samples with higher V_2O_5 ratio, i.e. 0.55V-0.45LB and 0.60V-0.40LB, had higher crystallinity as the prominence of Bragg's peak observed in their normallised XRD patterns. These two higher-crystallinity samples were then not longer off interest for further study. Samples were crushed into a small particle for morphology investigation. Small amount of powder was immersed in hexane to avoid moisture attack, which is normal for various borate glasses. The mixtures were ultra-sonicated and drop onto the TEM lazy carbon grid for further investigation. Thin area of the

crushed samples was also observed under high-resolution transmission electron microscopy (JEM-2000FC) to confirm the nature of the samples.

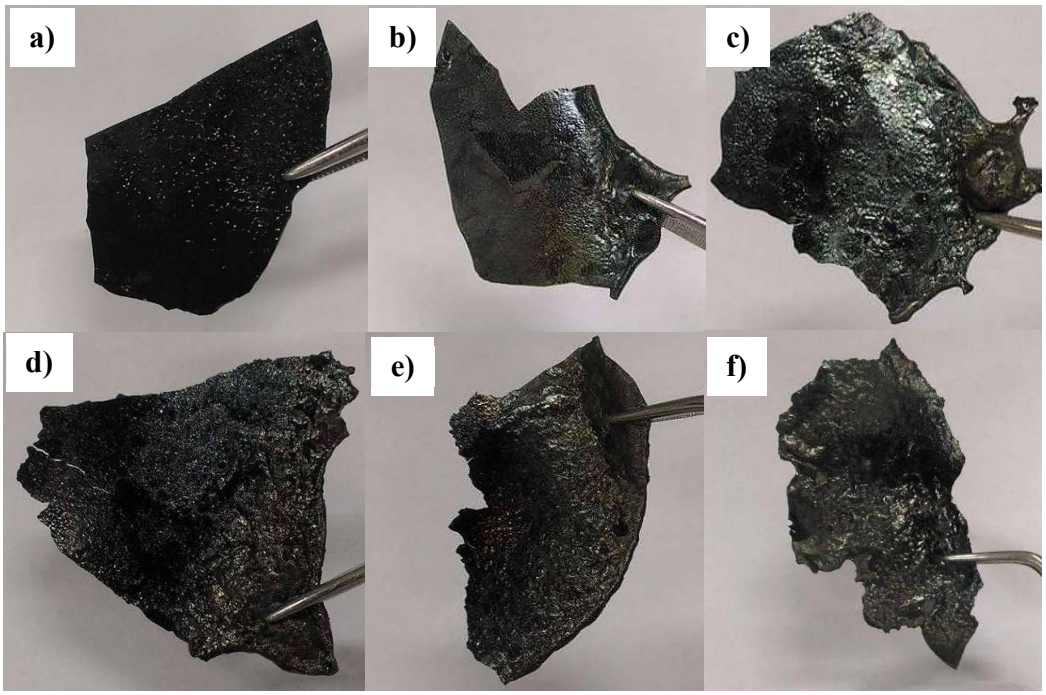

Figure 13 Samples obtained from melt-quench method, in which the V_2O_5 content in glass was **a)** 35, **b)** 40, **c)** 45, **d)** 50, **e)** 55 and **f)** 60 mol%.

From XRD patterns showed in **Figure 14**, it was obvious that the 55 and 60 mol% V_2O_5 containing samples were highly crystallised, especially 60% mol V_2O_5 sample, where the Bragg's peaks appear at approximately 13.9, 23.3, 27.6, 28.4, 30.8, 40.8 and 42.1 degree. The majority of the crystalline phase found in the melt-quench sample was lithium vanadate (LiV_3O_8), in which its XRD pattern was compared in **Figure 14**. It was clear that the samples with low vanadium oxide content, i.e. 35 to 50 mol%, showed most of the amorphous nature where Bragg's peak was not obviously detected. Thus, the samples with V_2O_5 content between 35 to 50 mol% were selected for further studies.

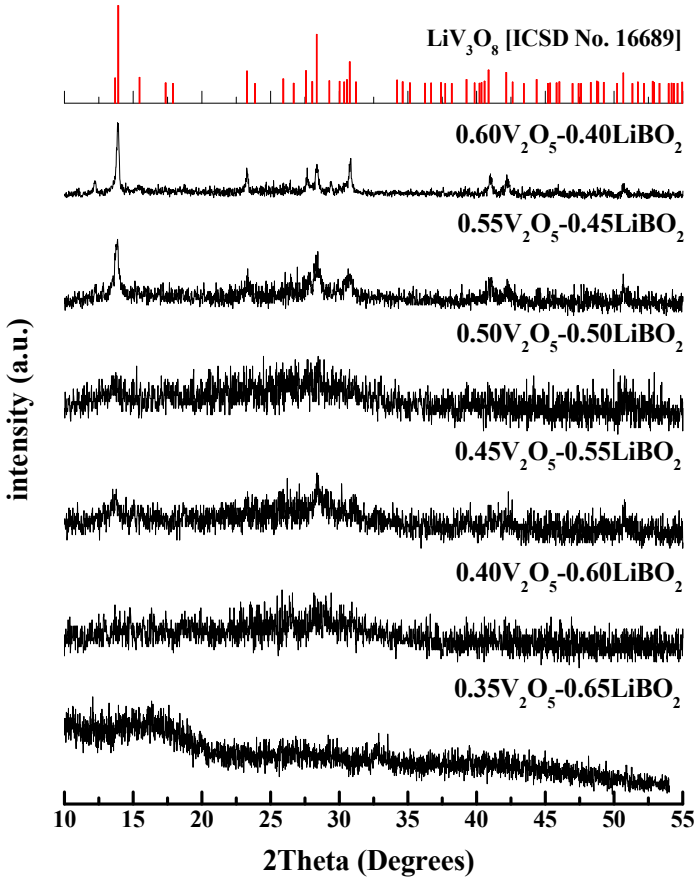

Figure 14 XRD patterns of samples obtained from melt-quench method having different V_2O_5 concentration

The thin edge of sample particles were magnified 300K times to observe the morphology of the samples. It was found that nanocrystalline phases (arrowed) have been found, in which the crystal size depending on the vanadium content. It seems likely that the larger amount of vanadium, the larger the crystalline size is as can be compared in **Figure 15**. The lattice fringes found might be the LiV_3O_8 crystallite phases as detected by XRD.

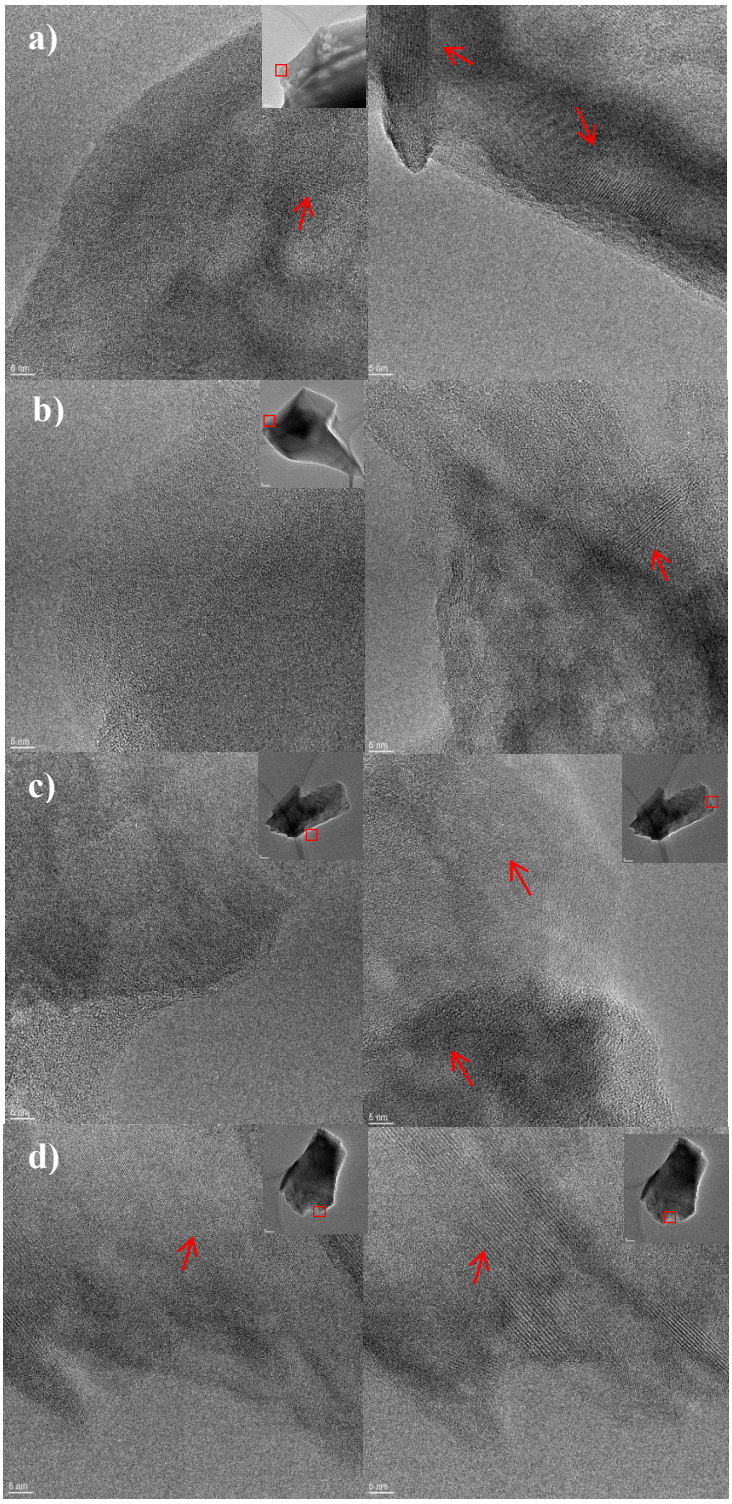

Figure 15 High resolution electron images of samples with different V_2O_5 content, i.e. a) 35, b) 40, c) 45 and d) 50 mol%, at 300000 times magnification.

The density and molar volume values of samples were plotted in **Figure 16** showing the increase of both as V_2O_5 content increases. The increase of densities of samples was dominate from the increment of high atomic mass fraction of vanadium oxide, which was similar to the bismuth borate glasses. However, in this study, the increase of MV as V_2O_5 content increases maybe due to the containing of large capacity of boron and vanadium environments, i.e. tetragonal boron; $[BO_4]^-$. Moreover, this may be due to the higher concentration of non-bridging oxygen (NBO) in the samples as more creation of ionic bonds leading the expansion of molar volume in the sample.

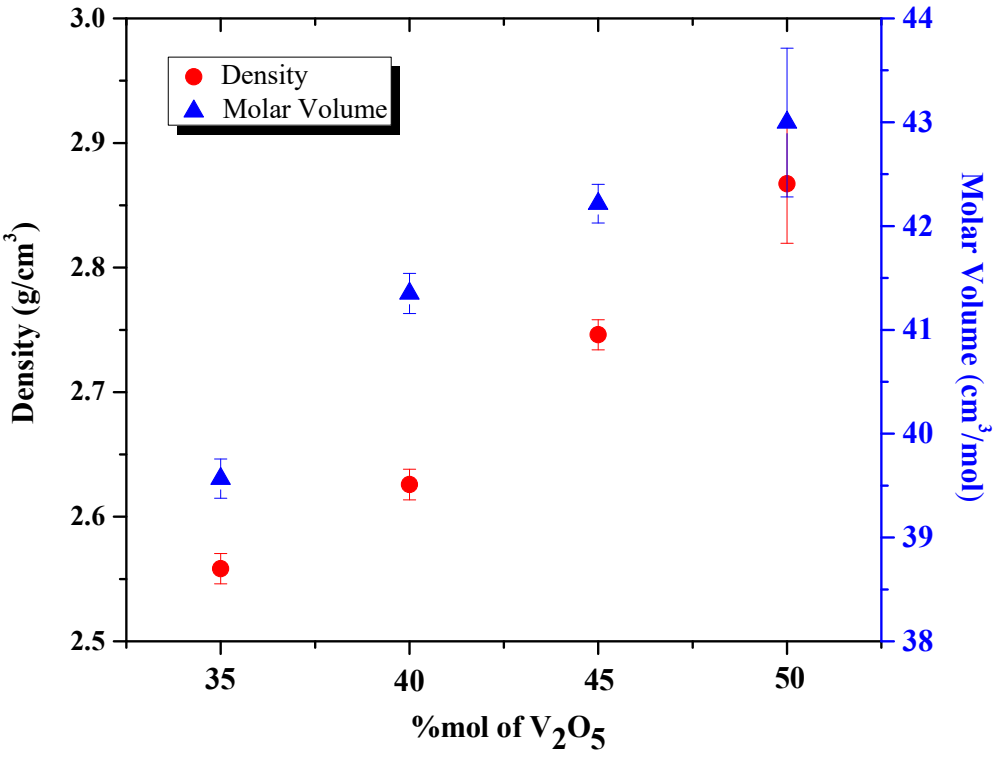

Figure 16 Densities and molar volumes relationships of samples with 35 – 50 mol% V_2O_5

Raman spectra shows in **Figure 16** demonstrating the change of glass structure. The interpretation of each peaks observed was also listed in **Table 7**. Peaks at the shift position of 154 cm^{-1} and 245 cm^{-1} corresponded to the vibration of a short bond of vanadium and oxygen in the sample, which could be found in the samples containing more than 40% vanadium oxide. Vibration of boron and oxygen bond in $[BO_4]^-$ in diborate superstructural unit was also detected at the corresponding Raman shift at 517 cm^{-1}. The peak can also be due to the vibration of V-O-V bond. The intensity at this position was stronger as vanadium content increases. The shift at 715 $cm^{-1}$is due to the vibration of B-O-B bond in metaborate superstructural unit containing $[BO_3]$. Peak at 765 cm^{-1} is a symmetric vibration of six membered ring structure containing one or two $[BO_3]$ units. Peak ranges from 916 cm^{-1} to 998 cm^{-1} was corresponding to the vibration of orthoborate group, which was found in glasses with vanadium content lover than 35 mol%. Finally, at 1020 cm^{-1}, vibrational of V^{5+}=O was assigned.

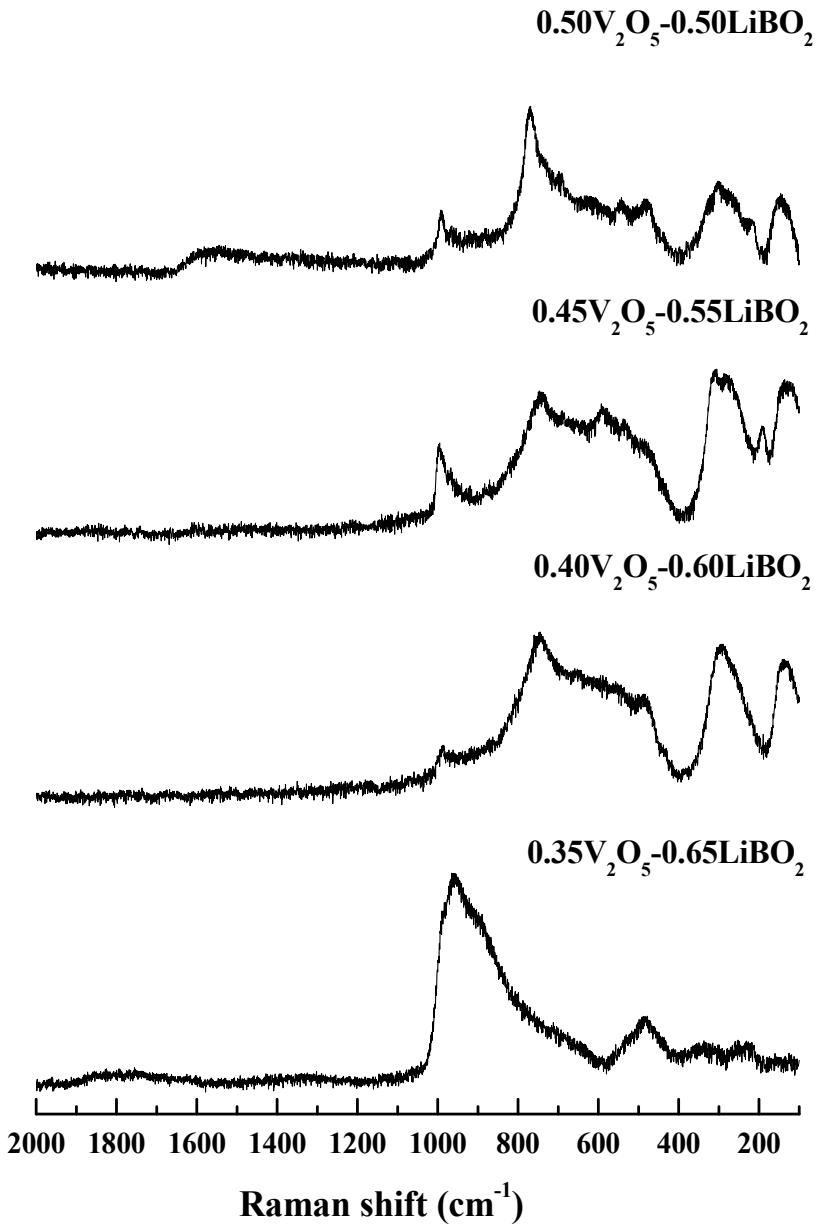

Figure 16 Raman spectra of samples with 35 – 50 mol% V_2O_5

Table 7 Raman shift lists with their assignments

Raman Shift (cm^{-1})	Assignments
154 และ 245	Vibration of short bond V-O
315	N/A
485	N/A
517	Vibration of diborate/(BO_4) or V-O-V
715	Vibration of B-O-B in metaborate
765	Symmetric vibration of six-membered ring with one or two [BO_3]
916-998	Vibration of B-O-B in orthoborate
1020	Vibration of V^{5+}=O (Double bond)
1520	N/A
1830	N/A

References

[1] D.W. Hall, M.A. Newhouse, N.F. Borrelli, W.H. Dumbaugh, D.L. Weidman, Nonlinear optical susceptibilities of high-index glass, *Applied Physics Letters*, **54** (1989) 1293-1295.

[2] A.S.L. Gomes, E.L.F. Filho, C.B. de Araujo, D. Rativa, R.E. de Araujo, K. Sakaguchi, F.P. Mezzapesa, I.C.S. Carvalho, P.G. Kazansky, Third-order nonlinear optical properties of bismuth-borate glasses measured by conventional and thermally managed eclipse Z scan, *Journal of Applied Physics*, **101** (2007) 033115-033117.

[3] R. Becker, *Lone-pair cations - A novel route to new low-dimensional materials*, Thesis in: Department of Inorganic Chemistry, Stockholm University, 2005.

[4] A.C. Hannon, E.R. Barney, D. Holland, The structure of tin borate based glasses, *Physics and Chemistry of Glasses-European Journal of Glass Science and Technology Part B*, **50** (2009) 271-283.

[5] N.S. Krasheninnikova, I.V. Frolova, O.V. Kaz'mina, A Method for Preparing Homogeneous Glass Batch*, Glass and Ceramics*, **61** (2004) 173-174.

[6] Z. Pan, S.H. Morgan, B.H. Long, Raman scattering cross-section and non-linear optical response of lead borate glasses, *Journal of Non-Crystalline Solids*, **185** (1995) 127-134.

[7] I.I. Oprea, H. Hesse, K. Betzler, Optical properties of bismuth borate glasses, *Optical Materials*, **26** (2004) 235-237.

[8] J. Kobelke, K. Schuster, D. Litzkendorf, A. Schwuchow, J. Kirchhof, V. Tombelaine, H. Bartelt, P. Leproux, V. Couderc, A. Labruyere, R. Jamier, Highly germanium and lanthanum modified silica based glasses in microstructured optical fibers for non-linear applications, *Optical Materials*, **32** (2010) 1002-1006.

[9] G. Yankov, L. Dimowa, N. Petrova, M. Tarassov, K. Dimitrov, T. Petrov, B.L. Shivachev, Synthesis, structural and non-linear optical properties of TeO_2–GeO_2–Li_2O glasses, *Optical Materials*, **35** (2012) 248-251.

[10] P.J. Bray, Nuclear magnetic resonance studies of glass structure, *Journal* of Non-Crystalline Solids, **73** (1985) 19-45.

[11] J. Swenson, L. Borjesson, W.S. Howells, Structure of borate glasses from neutron diffraction experiments, *Physical Review B*, **52** (1995) 9310-9319.

[12] B.N. Meera, J. Ramakrishna, Raman spectral studies of borate glasses, *Journal of Non-Crystalline Solids*, **159** (1993) 1-21.

[13] D.H. Lee, D.Y. Han, Characterization of borate glasses using solid-state nutation NMR, *Journal of the Korean Physical Society*, **32** (1998) 93-96.

[14] N. Laorodphan, *Structural Studies of Thallium containing germanate and borate glasses and crystalline phases*, Ph.D. Thesis in: Department of Physics, The University of Warwick, 2013.

[15] D. Holland, A.C. Hannon, M.E. Smith, C.E. Johnson, M.F. Thomas, A.M. Beesley, The role of Sb^{5+} in the structure of Sb_2O_3-B_2O_3 binary glasses - an NMR and Mossbauer spectroscopy study, *Solid State Nuclear Magnetic Resonance*, **26** (2004) 172-179.

[16] E.R. Barney, A.C. Hannon, N. Laorodphan, R. Dupree, D. Holland, A neutron diffraction and Tl-205 NMR study of the thallium germanate glass system, *Journal of Non-Crystalline Solids*, **356** (2010) 2517-2523.

[17] E.R. Barney, A.C. Hannon, N. Laorodphan, D. Holland, Influence of Lone-Pair Cations on the Germanate Anomaly in Glass, *Journal of Physical Chemistry C*, **115** (2011) 14997-15007.

[18] J.F. Bent, A.C. Hannon, D. Holland, M.M.A. Karim, The structure of tin silicate glasses, *Journal of Non-Crystalline Solids*, **232–234** (1998) 300-308.

[19] C.E. Stone, A.C. Wright, R.N. Sinclair, S.A. Feller, M. Affatigato, D.L. Hogan, N.D. Nelson, C. Vira, Y.B. Dimitriev, E.M. Gattef, D. Ehrt, Structure of bismuth borate glasses, *Physics and Chemistry of Glasses*, **41** (2000) 409-412.

[20] A. Bajaj, A. Khanna, B. Chen, J.G. Longstaffe, U.W. Zwanziger, J.W. Zwanziger, Y. Gómez, F. González, Structural investigation of bismuth borate glasses and crystalline phases, *Journal of Non-Crystalline Solids*, **355** (2009) 45-53.

[21] B.B. Sun, Y.B. Wang, J. Wen, H. Yang, M.L. Sui, J.Q. Wang, E. Ma, Artifacts induced in metallic glasses during TEM sample preparation, *Scripta Materialia*, **53** (2005) 805-809.

[22] M. Ishimaru, A. Hirata, M. Naito, Electron diffraction study on chemical short-range order in covalent amorphous solids, *Nuclear Instruments and Methods in Physics Research Section B: Beam Interactions with Materials and Atoms*, **277** (2012) 70-76.

[23] M.A. Bursukova, E.P. Kashchieva, Y.B. Dimitriev, Electron diffraction study of the short-range order in glasses of the system TeO_2-B_2O_3, *Journal of Non-Crystalline Solids*, **192–193** (1995) 40-44.

[24] D.J. Barber, Radiation damage in ion-milled specimens: characteristics, effects and methods of damage limitation, *Ultramicroscopy*, **52** (1993) 101-125.

[25] B.J. Kestel, Preparation of damage-free glass TEM specimens, *Ultramicroscopy*, **83** (2000) 61-66.

Conclusions and Outputs

Conclusions

- **Tin borate glass**

1. The glass was not successfully prepared due to the limitation of the furnace.

- **Bismuth borate glasses**

1. The X-ray diffraction and high resolution electron image revealed that the samples were amorphous.

2. The density values of glasses increased as bismuth oxide content increases. However, anomaly of molar volume was detected.

3. Inconclusive result was obtained from electron diffraction technique due to the limitation of the interpretation technology and software

4. Raman spectra showed the reduction of 3-coordinated boron.

- **Lithium doped vanadium borate glasses**

1. All samples were partially crystallised as the nano crystallites, which can be confirmed by X-ray diffraction and high resolution electron images.

2. Density values of the lithium doped vanadium borate glasses increased as vanadium oxide content increases. However, the molar volumes of the glasses also increased.

3. Higher concentration of 4-coordinated boron in the glass structure increases as vanadium oxide content increases.

Outputs

1. International Journal Publication

Manuscript for Journal of Alloys and Compounds (*In preparation*)

2. Research Utilization and Application

n/a